

CAN DIRECT COLLAPSE BLACK HOLES LAUNCH GAMMA-RAY BURSTS AND GROW TO SUPERMASSIVE BLACK HOLES?

TATSUYA MATSUMOTO¹, DAISUKE NAKAUCHI^{1,2}, KUNIHITO IOKA^{3,4}, ALEXANDER HEGER^{5,6,7} AND TAKASHI NAKAMURA¹
Draft version July 23, 2018

ABSTRACT

The existence of black holes (BHs) of mass $\sim 10^9 M_\odot$ at $z \gtrsim 6$ is a big puzzle in astrophysics because even optimistic estimates of the accretion time are insufficient for stellar mass BHs of $\sim 10 M_\odot$ to grow into such supermassive BHs. A resolution of this puzzle might be the direct collapse of supermassive stars with mass $M \sim 10^5 M_\odot$ into massive seed BHs. We find that if a jet is launched from the accretion disk around the central BH, the jet can break out the star because of the structure of the radiation pressure-dominated envelope. Such ultra-long gamma-ray bursts with duration of $\sim 10^4$ - 10^6 s and flux of 10^{-11} - 10^{-8} erg s⁻¹ cm⁻² could be detectable by *Swift*. We estimate an event rate of $\lesssim 1$ yr⁻¹. The total explosion energy is $\gtrsim 10^{55}$ - 10^{56} erg. The resulting negative feedback delays the growth of the remnant BH by about 70 Myr or evacuates the host galaxy completely.

1. INTRODUCTION

Gamma-ray bursts (GRBs) are among the most violent explosions in the Universe. They are classified into two populations by the duration of prompt emission T_{90} : short GRBs (SGRBs) with $T_{90} < 2$ s and long GRBs (LGRBs) with $T_{90} > 2$ s (Kouveliotou et al. 1993). A widely accepted model of LGRBs is the collapsar scenario, in which a black hole (BH) and accretion disk system is formed after the stellar collapse, and launches a relativistic jet that breaks out the progenitor star, producing a GRB (Woosley 1993; MacFadyen & Woosley 1999). Theoretical models identify the typical duration of a LGRB ($T_{90} \sim 30$ s) as the free-fall time of the envelope, or the sound-crossing time of the shocked envelope, of a Wolf-Rayet (WR) star (Mizuta & Ioka 2013). From observation we know that at least some LGRBs are accompanied by broad-lined Ic supernovae (SNe; Woosley & Bloom 2006; Hjorth & Bloom 2012). This suggests a tight connection between GRBs and progenitors with stripped envelope like WR stars.

Recently, some LGRBs have been discovered to show ultra-long duration of the prompt emission with $\delta t_\gamma \sim 10^4$ s. These have been named ultra-long gamma-ray bursts (ULGRBs) (Gendre et al. 2013; Levan et al. 2014). The ultra-long duration was first predicted in the context of Population III (PopIII) GRBs (Suwa & Ioka 2011; Nagakura et al. 2012), and subsequent studies suggested that a metal-poor blue supergiant (BSG) col-

sar rather than the WR one is more favorable to explain such bursts (Gendre et al. 2013; Kashiyama et al. 2013; Nakauchi et al. 2013). Since metal-poor stars may suffer from little mass loss, metal-poor BSG stars would keep massive hydrogen envelopes until the precollapse phase (Woosley et al. 2002). Therefore, the accretion of the massive hydrogen envelope can lead to the long-lasting central engine activity (Suwa & Ioka 2011; Nagakura et al. 2012; Quataert & Kasen 2012; Woosley & Heger 2012; Nakauchi et al. 2013). Since metal-poor stars are considered to be the dominant population in the high- z Universe, ULGRBs might be a dominant population of GRBs in the high- z Universe (e.g., de Souza et al. 2011).

On the other hand, the existence of BHs of mass $\sim 10^9 M_\odot$ at $z \gtrsim 6$ (Fan 2006; Mortlock et al. 2011; Wu et al. 2015) is a great mystery in astrophysics because the accretion time is not enough to grow the BHs from the stellar mass BHs of mass $\sim 10 M_\odot$ (e.g., Haiman 2013). Many attempts are made to solve this problem. One possible solution may be the formation from PopIII stars. Recent numerical simulations suggest that the mass of PopIII stars reaches up to $10^{2-3} M_\odot$ (Hirano et al. 2014; Susa et al. 2014). BHs born from these PopIII stars can barely grow up to supermassive BHs of mass $10^9 M_\odot$ at $z \gtrsim 6$, if successive high mass accretions are maintained. Feedback effects from accreting BHs, however, decrease the accretion rate (Alvarez et al. 2009). Thus it seems difficult for seed BHs from PopIII stars to form the observed supermassive BHs without resorting to super-Eddington accretion via such as Bondi and cold accretion (e.g., Volonteri & Rees 2005; Gaspari et al. 2013) or efficient mergers (e.g., Madau & Rees 2001).

An attractive alternative might be the formation of supermassive stars (SMSs) of mass $\sim 10^5 M_\odot$. SMSs may be formed in the high temperature region irradiated by the strong ultra-violet radiation from nearby galaxies (Omukai 2001; Bromm & Loeb 2003; Shang et al. 2010; Latif et al. 2013; Inayoshi et al. 2014; Johnson et al. 2014). When SMSs end their life due to the exhaustion of their nuclear fuel or the general relativistic (GR) instability (Chandrasekhar 1964; Osaki 1966;

¹ Department of Physics, Kyoto University, Kyoto 606-8502, Japan

² Astronomical Institute, Tohoku University, Aoba, Sendai 980-8578, Japan

³ Theory Center, Institute of Particle and Nuclear Studies, KEK, Tsukuba 305-0801, Japan

⁴ Department of Particle and Nuclear Physics, SOKENDAI (The Graduate University for Advanced Studies), Tsukuba 305-0801, Japan

⁵ Monash Centre for Astrophysics, Monash University, Melbourne, Victoria 3800, Australia

⁶ University of Minnesota, School of Physics and Astronomy, Minneapolis, MN 55455, USA

⁷ Shanghai Jiao-Tong University, Center for Nuclear Astrophysics, Department of Physics and Astronomy, Shanghai 200240, P. R. China

Shapiro & Teukolsky 1983; Shibata & Shapiro 2002), they collapse to massive BHs of mass $\sim 10^5 M_\odot$, so-called direct collapse BHs (DCBHs). If these DCBHs are seeds, the accretion time might be enough to grow the BHs to $\sim 10^9 M_\odot$ at $z \gtrsim 6$.

Various violent phenomena from the gravitational collapse of SMSs are expected such as the energetic neutrino bursts (Fryer & Heger 2011) and SNe with very huge explosion energy of $\sim 10^{55}$ erg (Johnson et al. 2013; Whalen et al. 2013; Chen et al. 2014). In this paper, we consider ULGRBs from SMSs as another possibility. If SMSs evolve without mass ejection and collapse to form BH-disk systems, like collapsars, we can expect the launch of the relativistic jet similar to LGRBs⁸. Since SMSs are larger in radius than PopIII first stars of mass 10-1000 M_\odot or BSGs, we expect that the duration of ULGRBs is even longer than that of the observed ULGRBs. The detection of such ULGRBs would enable us to observe the very moment of the birth of first quasars to probe the high- z Universe. Such energetic explosions might prevent the subsequent gas accretion and the growth of the DCBHs. Thus, it is worth evaluating the details of relativistic jet explosions from supermassive collapsars and their observational signatures.

This paper is organized as follows: In §2, we show the pre-collapse stellar models of SMSs, which evolve from zero age main sequence (ZAMS) stars. In §3, we describe the method to calculate the jet dynamics in the SMS envelope. In §4, we show that the jet can break out the SMS. We also discuss the observational signatures and the detectability of GRBs from supermassive collapsars. In §5, we discuss the other progenitor model in which the SMS is accreting mass and collapses through the GR instability. Then we estimate the event rate of GRBs from SMSs, and discuss the effects of GRBs on their environment. A summary and our conclusions are given in §6. Throughout this paper, we consider the Λ CDM cosmology and adopt the cosmological parameters as : $H_0 = 67.8 \text{ km s}^{-1} \text{ Mpc}^{-1}$, $\Omega_m = 0.308$ and $\Omega_\Lambda = 0.692$ (Planck Collaboration et al. 2015).

2. PROGENITOR MODEL

Theoretical studies of the primordial star formation have suggested that SMSs with $\gtrsim 10^5 M_\odot$ can be formed under the hot environments of first galaxies (Omukai 2001; Bromm & Loeb 2003; Shang et al. 2010; Latif et al. 2013; Inayoshi et al. 2014; Johnson et al. 2014). Whereas molecular hydrogen is the primary coolant in primordial star-forming clouds, its formation is prevented under strong ultra-violet radiation from nearby galaxies, so that the temperature is kept at $\sim 10^4 \text{ K}$ in such a cloud due to the hydrogen atomic cooling. The accretion rate onto a protostar \dot{M} can be evaluated by dividing the Jeans mass M_J of the

star-forming cloud by the free-fall time t_{ff} :

$$\dot{M} \sim M_J/t_{\text{ff}} \sim c_s^3/G \sim 0.51 \left(\frac{T}{10^4 \text{ K}} \right)^{3/2} M_\odot \text{ yr}^{-1}, \quad (1)$$

where c_s and T are the sound velocity and the temperature of the cloud, and G is the gravitational constant, respectively. We also assume that the cloud is composed of only hydrogen, for simplicity. Thus, the mass accretion rate onto the protostar formed in the central region of the star-forming cloud can be as high as $\sim 0.1\text{-}1 M_\odot \text{ yr}^{-1}$ under such hot environments. The protostar can grow up to a SMS with $\gtrsim 10^5 M_\odot$ within its lifetime of $\sim 1 \text{ Myr}$ through such a high mass accretion rate.

When the mass accretion onto the protostar stops because of radiation feedback, or for other reasons, the protostar contracts onto the ZAMS in a Kelvin-Helmholtz timescale. Since the SMSs are almost fully convective and the Kelvin-Helmholtz timescale is short compared to the lifetime of the star, the resulting final stellar structure should be the same as long as accretion stops not too close to hydrogen depletion. After the SMS runs through its nuclear burning phases⁹, it collapses to a BH similar to a massive star¹⁰. When the SMS collapses to a BH, it may produce a GRB by launching a relativistic jet provided there is enough angular momentum. Thus, we adopt this pre-collapse SMS for our progenitor model.

In this paper, we focus on a supermassive progenitor with a ZAMS mass of $10^5 M_\odot$, but for comparison also consider a progenitor which has the ZAMS mass of $10^4 M_\odot$ (Fryer & Heger 2011). We call the former model as “1E5 model” and the latter model as “1E4 model”, respectively. The density profiles of these pre-collapse SMSs are shown in Figure 1. We can see that they have very large radii of $R_* \sim 10^{14} \text{ cm}$, which are as large as those of present-day RSGs (green curve in Fig. 1). Note that the envelopes of the SMS models have steeper density profiles ($\rho \propto r^{-3}$) than that of the RSG model ($\rho \propto r^{-3/2}$). This is because radiation pressure dominates in the SMS envelopes while gas pressure dominates in the RSG envelope (see Section 4.1).

It is not trivial whether the relativistic jet can break out the envelope of the supermassive progenitors successfully since it can not break out the large envelope of RSGs (Matzner 2003; Suwa & Ioka 2011; Nakauchi et al. 2012). Suwa & Ioka (2011); Nagakura et al. (2012) studied relativistic jet explosions from massive PopIII stars ($M_* \simeq 10^3 M_\odot$), and found that the jet breakout is possible despite the large radius of $R_* \sim 10^{13} \text{ cm}$. They attributed this to the long duration of the mass accretion of the massive envelope. In this paper, we consider supermassive PopIII stars which have $M_* \simeq 10^4\text{-}10^5 M_\odot$ and $R_* \sim 10^{14} \text{ cm}$ to determine whether the jet can break out of the envelope. These stars have 10 times larger radii compared to the massive PopIII stars considered by Suwa & Ioka (2011); Nagakura et al. (2012) so that the jet might not break out the envelope.

3. NUMERICAL METHOD

3.1. Jet Model

⁸ When a SMS collapse to a BH, there is some possibility that a quasi-star, which is powered by the central BH accretion, could form (Begelman et al. 2008). In this work, however, we consider that the central BH launches a jet as ordinary GRBs. Previous works (Barkov 2010; Czerny et al. 2012) did not consider the jet propagation in the SMS, so that the observed quantities such as the luminosity and duration are unable to obtain.

⁹ The advanced phases may be accelerated as part of the collapse.

¹⁰ Even a phase with a hot proto-BH due to neutrino trapping as observed by Fryer et al. (2001) may nor occur.

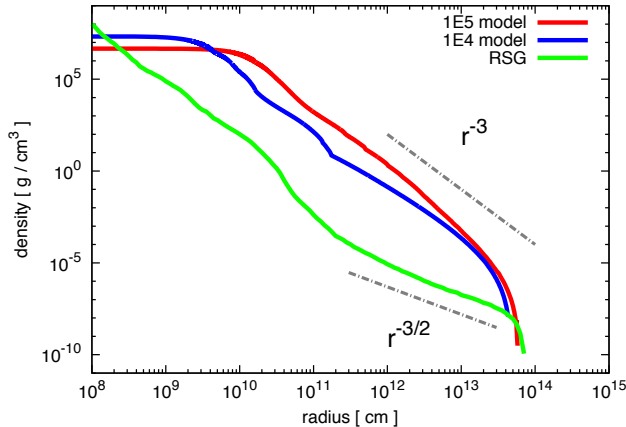


Figure 1. Density profiles of SMSs in their pre-collapse phase. The red curve and blue curve correspond to the 1E5 model and the 1E4 model, respectively. These profiles are obtained by calculating the metal-free $10^5 M_\odot$ and $10^4 M_\odot$ ZAMS stars until the nuclear fuels are exhausted in the center. The green curve shows the density profile of a RSG (pre-supernova structure of Model s15 from Woosley et al. 2002). These profiles show that SMSs have similar radii with a RSG but steeper density profile than that of a RSG. The gray dash-dotted lines show the slope of the power-law density profiles of $\rho \propto r^{-3}$ and $\rho \propto r^{-3/2}$ as references.

We adopt a simple jet model in which the jet luminosity varies with time and depends on the mass accretion rate onto the BH (Suwa & Ioka 2011). The SMS begins to collapse, when its nuclear fuel is exhausted in the center, and forms a massive BH. We evaluate the mass accretion rate onto the central BH using the free-fall timescale as typical timescale. For each mass shell at radius r and mass coordinate M_r , the free-fall timescale can be calculated from

$$t_{\text{ff}}(r) = \sqrt{\frac{3\pi}{32G\bar{\rho}}} = \frac{\pi}{2} \sqrt{\frac{r^3}{2GM_r}}, \quad (2)$$

where $\bar{\rho} = M_r / (\frac{4\pi}{3}r^3)$ is the mean density within r . The mass accretion rate is calculated by (Woosley & Heger 2012, 2015)

$$\dot{M} = \frac{dM_r}{dt_{\text{ff}}} = \frac{dM_r/dr}{dt_{\text{ff}}/dr} = \frac{2M_r}{t_{\text{ff}}(r)} \left(\frac{\rho}{\bar{\rho} - \rho} \right). \quad (3)$$

A relativistic jet will be launched from the central engine, which is composed of a BH and an accretion disk. The mechanisms of launching relativistic outflows are still uncertain, though several processes have been proposed such as MHD mechanism and neutrino-antineutrino annihilation mechanism (e.g., Blandford & Znajek 1977; Popham et al. 1999). Suwa & Ioka (2011) studied the jet-driven explosions from massive PopIII stars and found that the MHD mechanism works long enough for the jet to break out the envelope, whereas the neutrino mechanism does not. Therefore, we assume the MHD mechanism hereafter. In the MHD process, the jet luminosity can be modeled according to (Komissarov & Barkov 2010)

$$L_j(t) = \eta_j \dot{M}(t) c^2, \quad (4)$$

where η_j is the efficiency parameter. For simplicity we assume that η_j is constant. We can take into account the

effect of the progenitor rotation by adjusting the parameter value η_j . When a sufficiently fast-rotating progenitor collapses, it can form a BH and accretion disk system. The remainder of the star then falls onto the central BH in the accretion time t_{acc} , which can be related to the free-fall time as $t_{\text{acc}} \propto \frac{1}{\alpha} t_{\text{ff}}$, where α is the viscosity parameter (Shakura & Sunyaev 1973; Kumar et al. 2008). Thus, the factor α can be absorbed into the effective value of η_j . We use $\eta_j = 6.2 \times 10^{-4}$, which is calibrated to reproduce the total jet energy of typical LGRBs of $E_{\text{tot}} = \int \eta_j \dot{M} c^2 dt = 10^{52}$ erg for a WR progenitor model (Suwa & Ioka 2011).

Throughout this section, the time t is measured in the central engine frame. We set $t = 0$ as the time when the black hole is formed. Since the formation mechanism of a relativistic jet is still under debates, the time of jet formation, t_{in} , is also uncertain and should be a parameter of this study. Following the previous studies, we assume that the jet is formed when the mass of BH reaches $3 M_\odot$: $t_{\text{in}} = t_{\text{ff}}(r_{\text{in}})$, where the enclosed mass within the radius r_{in} is $3 M_\odot$, i.e., $M_{r_{\text{in}}} = 3 M_\odot$ (Suwa & Ioka 2011). The choice of t_{in} (or $M_{r_{\text{in}}}$), however, has little influence on the jet dynamics in the envelope as long as t_{in} is much smaller than the jet break out time. In fact, we find that the jet breakout time is within a factor of two, when the jet formation time is changed as $M_{r_{\text{in}}} = 30 M_\odot$, $300 M_\odot$, and $3,000 M_\odot$ in the 1E5 model.

3.2. Jet Propagation in the SMS Envelope

Here, we describe the jet dynamics in the progenitor envelope following the prescription in Matzner (2003); Suwa & Ioka (2011); Bromberg et al. (2011); Nakauchi et al. (2012). A relativistic jet launched from the central engine collides with the stellar matter and forms the shocked region at the jet head. The jet head is composed of the forward shock which sweeps the stellar matter and the reverse shock which decelerates the jet matter. Both shocked matter are divided by the contact discontinuity. Then the velocity of the jet head can be calculated from the pressure balance at the contact discontinuity as

$$\rho_j c^2 h_j \Gamma_j^2 \Gamma_h^2 (\beta_j - \beta_h)^2 + P_j = \rho_a c^2 h_a \Gamma_h^2 \beta_h^2 + P_a, \quad (5)$$

where, ρ , h , and P represent the mass density, specific enthalpy, and pressure measured in the fluid rest frame, respectively, and β and $\Gamma = (1 - \beta^2)^{-1/2}$ are the velocity normalized by the speed of light c and the Lorentz factor, respectively. The subscripts ‘‘h’’, ‘‘j’’, and ‘‘a’’ indicate that the quantity is measured in the rest frame of the jet head, the jet, and the ambient stellar medium, respectively. Since the stellar medium is composed of the non-relativistic matter, we can neglect its pressure against the rest mass energy density, i.e., $P_a \ll \rho_a c^2$, and this also leads to $h_a \simeq 1$. In the left hand side of Equation (5), we can also neglect the jet pressure, since the jet is ultra-relativistic ($\beta_j \simeq 1$ and $\Gamma_j \gg 1$).

Using the above approximations, the velocity of the jet head is given by

$$\beta_h \simeq \frac{1}{1 + \tilde{L}^{-\frac{1}{2}}}, \quad (6)$$

where $\tilde{L} = \rho_j h_j \Gamma_j^2 / \rho_a$ is a parameter which determines

the jet dynamics. Using the collimation-corrected jet luminosity given by

$$L_j = \rho_j c^3 h_j \Gamma_j^2 \beta_j \Sigma_h, \quad (7)$$

\tilde{L} is given by

$$\tilde{L} \simeq \frac{L_j}{\rho_a c^3 \Sigma_h}, \quad (8)$$

where Σ_h is the cross section of the jet head. Thus, \tilde{L} is the ratio of the luminosity of the jet to that of the ambient stellar medium rest energy flux. Here, we assume that the opening angle of the jet is constant with $\theta = 5^\circ$. This is the typical value obtained from the afterglow observations of LGRBs (Frail et al. 2001). Then the cross section can be given by $\Sigma_h = \pi(r_h \theta)^2$, where $r_h(t) = \int c \beta_h dt$ is the radius of the jet head.

As long as the velocity of the jet head is non-relativistic ($\beta_h < 1$), the shocked jet head can expand sideways to form a cocoon structure surrounding the jet. Since the temperature of the cocoon is high, it is radiation-pressure-dominated. As long as the sound crossing time in the cocoon is shorter than the dynamical time of the jet head, we can neglect the inner structure of the cocoon and assume that the cocoon is uniform. Hereafter, we consider the one-zone model for the lateral expansion of the cocoon. The cocoon is overpressured with respect to the ambient stellar medium so that it expands laterally. By considering pressure balance at the surface of the cocoon, the lateral expansion velocity of the cocoon is calculated by (Begelman & Cioffi 1989)

$$\beta_c = \sqrt{\frac{P_c}{\bar{\rho}_a c^2}}, \quad (9)$$

where P_c is the pressure in the cocoon and $\bar{\rho}_a(r_h) = M_{r_h}/(4\pi r_h^3/3)$ is the mean density of the progenitor star within the radius r_h .

Since the cocoon matter is radiation-pressure-dominated, the pressure is given by $P_c = E_c/3V_c$, where E_c and V_c represent the total energy and volume in the cocoon, respectively. Because the cocoon energy is supplied from the jet head, it is given by

$$E_c(t) = \eta_c \int_{t_{\text{in}}}^{t - \frac{r_h(t)}{c}} L_j(t') dt', \quad (10)$$

where η_c indicates the fraction of the jet luminosity streaming into the cocoon. Throughout the paper, we set $\eta_c = 1$, since the velocity of the jet head is non-relativistic for most of the time within the progenitor envelope. In Equation (10), the upper limit of the integral indicates that at t , the jet head receives the luminosity which is produced at $t - r_h(t)/c$ at the central engine. For the cocoon volume, we assume that the cocoon has a conical shape with the height of $r_h(t)$ and the base radius of $r_c(t)$, so that it is given by

$$V_c(t) = \frac{1}{3} \pi r_c^2(t) r_h(t), \quad (11)$$

where $r_c(t)$ is the lateral distance of the cocoon surface from the jet axis given by $r_c(t) = \int c \beta_c dt$.

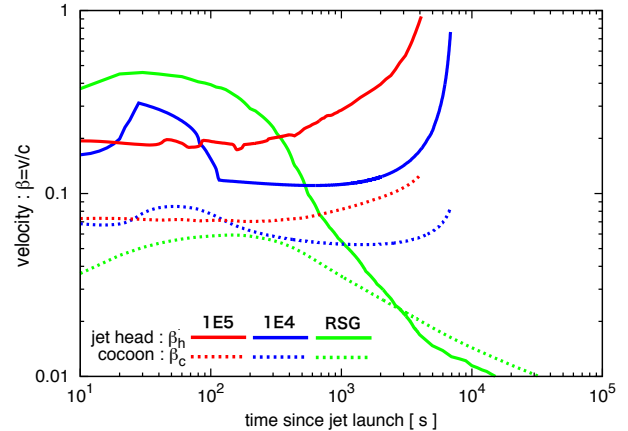


Figure 2. Time evolution of the velocities of the jet head and the lateral expansion of the cocoon surface. *Red, blue and green lines* correspond to the 1E5 model, the 1E4 model and the RSG, respectively. The horizontal axis shows the time from jet formation. The vertical axis shows the velocity divided by the speed of light. The *solid and dashed curves* correspond to the velocities of the jet head β_h and the cocoon surface β_c , respectively. For the 1E5 model and the 1E4 model, the jet head velocity is always larger than that of the cocoon edge so that the supermassive collapsar jet can break out the envelope. For $t \gtrsim 500$ s and $t \gtrsim 2,000$ s, the jet head is accelerated drastically in the 1E5 and 1E4 models, respectively, because the envelope density decreases more steeply than $\propto r^{-3}$. On the other hand, in the RSG, the jet head velocity is overtaken by that of the cocoon at $\sim 3,000$ s.

Substituting Equations (4) and (8) and the definition of Σ_h into Equation (6), the jet head velocity is given by

$$\beta_h \simeq \left[1 + \left(\frac{\pi c \theta^2 \rho_a(r_h) r_h^2}{\eta_j \dot{M}(t)} \right)^{1/2} \right]^{-1}. \quad (12)$$

Substituting Equations (10) and (11) into (9), the lateral expansion velocity of the cocoon is given by

$$\beta_c \simeq \frac{2r_h}{cr_c} \left[\frac{\eta_c \int_{t_{\text{in}}}^{t - \frac{r_h}{c}} L_j(t') dt'}{3(M_{r_h} - M_{r_{\text{in}}})} \right]^{1/2}. \quad (13)$$

4. ULGRBS FROM SUPERMASSIVE COLLAPSARS

4.1. Successful Breakout of Supermassive Collapsar Jets

In Figure 2, we show the time evolution of the velocities of the jet head and the lateral expansion of the cocoon surface with solid and dashed curves, respectively. Each color corresponds to the 1E5 model (red), the 1E4 model (blue), and the RSG model (green), respectively. They are calculated from Equations (12) and (13). The horizontal axis shows the time from jet formation: $t - t_{\text{in}}$. The vertical axis shows the velocity divided by the speed of light.

We can see that for the models 1E4 and 1E5, the velocity of the jet head is always larger than that of the cocoon surface. On the other hand, for the RSG model, the velocity of the cocoon exceeds that of the jet head at $\gtrsim 3,000$ s. In the latter case, the radius of the jet head is comparable to the lateral size of the cocoon surface so that they can reach the stellar surface almost at the same time. This looks like a spherical explosion rather than a

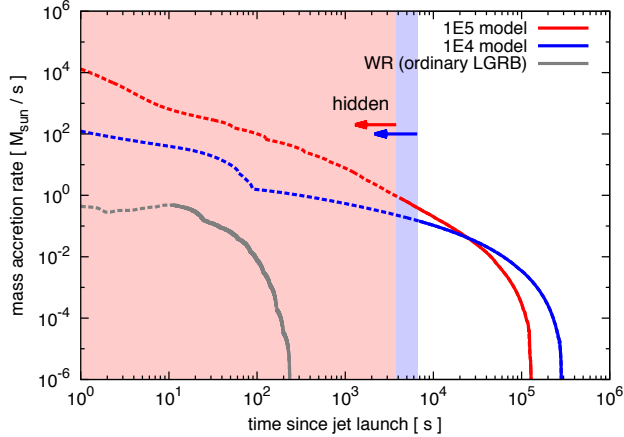


Figure 3. Time evolution of the mass accretion rate onto the BH. The horizontal axis is the time from jet formation. The red and the blue lines corresponds to the accretion rate obtained from the 1E5 model and the 1E4 model, respectively. Whole in each color, dashed and solid lines correspond to the time before and after the jet breakout, respectively. The shaded region in each color means that the jet head propagates in the progenitor’s interior and the jet is “hidden” from the observers. The accretion rate obtained from the WR model corresponding to LGRBs is shown by the gray curve as a reference. We can see that supermassive collapsar jets can lead to ULGRBs with the duration of $T_{90} \sim 10^4$ s up to $\gtrsim 10^5$ s. Note that the light curves decline steeply after the breakout, so that the observed duration T_{90} is approximately equal to the breakout time.

collimated explosion. On the other hand, in the former case, the collimated jet breaks out the progenitor surface since the jet head reaches the surface much earlier than the cocoon.

In Figure 3, we show the time evolution of the mass accretion rate onto the BH. The horizontal axis represents the time from jet formation. The red and blue curves correspond to the accretion rate obtained from the 1E5 model and the 1E4 model, respectively. While on each curve, dashed and solid regions correspond to the time before and after the jet breakout, respectively. We also show the accretion rate obtained from the WR model (i.e., LGRB) with the gray curve as a reference. We can see that supermassive collapsar jets can lead to ULGRBs with the duration of $\gtrsim 10^5$ s, owing to the accretion of the massive envelope.

While the SMS models have as large radii as present-day RSGs, we find that the relativistic jet can break out the progenitor envelope successfully. This can be attributed to the difference in the slope of the density profile. At the outer envelope of a polytropic star with the polytropic index n , the density profile can be approximated as $\rho_a(r) \propto (R_*/r - 1)^n \sim r^{-n}$ (Matzner & McKee 1999). Since SMSs have radiation-pressure-dominated convective envelopes, the index can be approximated as $n = 3$ (Shapiro & Teukolsky 1983; Kippenhahn & Weigert 1990). On the other hand, RSGs have gas-pressure-dominated convective envelopes so that the index is $n = 1.5$. Thus, the SMS models have steeper density profiles than the RSG models.

When the velocity of the jet head is non-relativistic, \tilde{L} is less than unity, so that the velocity can be approxi-

mately evaluated as

$$\beta_h(t) \sim \tilde{L}(t)^{1/2} \propto \dot{M}(t)^{1/2} r_h(t)^{\frac{n-2}{2}}. \quad (14)$$

Furthermore, by using that \dot{M} is approximated as $\dot{M}(t) \propto t^{\frac{3-2n}{3}}$ in the density profile of $\rho_a(r) \propto r^{-n}$ (Suwa & Ioka 2011), and that r_h is evaluated roughly as $r_h \propto \beta_h t$, we obtain

$$\beta_h(t) \propto r_h(t)^{\frac{n-3}{9-2n}}, \quad (15)$$

from Equation (14). Therefore the jet head is accelerated in the outer region of the SMS envelopes where the density profile decreases more steeply than $\propto r^{-3}$. On the other hand, the jet head is decelerated in the RSG envelopes. From Figure 2, we can see that the jet heads are accelerated drastically at $t \gtrsim 500$ s and $t \gtrsim 2,000$ s for the 1E5 and 1E4 models, respectively, when the jet heads enter the regions where the envelope density decreases more steeply than $\propto r^{-3}$. On the other hand, for RSGs, the velocity of the jet head is decelerated in the envelope so that it takes much longer time to break out the envelope. In this case, the lateral size of the cocoon becomes comparable to the radius of the jet head. This is a spherical explosion but not a collimated GRB. Thus, RSGs cannot be the progenitor of LGRBs as shown by Matzner (2003); Suwa & Ioka (2011); Nakauchi et al. (2012).

It is possible that a disk wind flows out isotropically from the accretion disk and changes the envelope structure. In this case, the disk wind and the deformed envelope may affect the jet propagation. Unless the wind velocity v_w is larger than the jet head and cocoon velocity, however, this effect can be ignored. The wind velocity is evaluated from the wind energy as $E_w \sim M_w v_w^2/2$, where M_w is the mass of the wind component. The wind energy is also given by $E_w \sim \int \eta_w \dot{M} c^2 dt$, where η_w is the efficiency parameter, as defined for the jet luminosity in Equation (4). On the other hand, the cocoon velocity is evaluated by $E_c \sim M_c v_c^2/2 \sim \int \eta_j \dot{M} c^2 dt$. From these equations, we obtain the ratio of the cocoon velocity to the wind velocity as $v_c/v_w \sim (M_w \eta_j / M_c \eta_w)^{1/2}$. In our work, the jet efficiency parameter is $\eta_j \sim 6 \times 10^{-4}$. As the wind flows out isotropically while the cocoon expands around the jet, their masses are related as $M_c \sim M_w \theta^2/2$, where $\theta \sim 0.1$ is the jet opening angle. Then, we have $v_c/v_w \sim 0.3 \eta_w^{-1/2}$. Thus, when the disk wind flows out very efficiently ($\eta_w \gtrsim 0.1$), we should consider the effect of the isotropic wind outflow on the envelope structure and the jet propagation. The recent numerical simulations of super-Eddington accretion disks suggest the value of $\eta_w \sim 0.01$ (Jiang et al. 2014)¹¹, which yields $v_c \sim 3v_w$. It should be noted that the accretion rates in their simulations are $\dot{M} \sim 100 L_{\text{Edd}}$, while in our situation, the mass accretion rates amount to $\dot{M} \gtrsim 10^{10} L_{\text{Edd}}$. We need numerical calculations in order to study the disk wind in our case.

4.2. Prompt emission

¹¹ Sądowski et al. (2014) also gives the efficiency ~ 0.3 , although this value includes the efficiency from the accretion energy to the radiation and magnetic energy.

Once the relativistic jet breaks out the progenitor's envelope, it can contribute to the prompt high-energy emission, like LGRBs. Here, we evaluate the observational signatures and the detectability of the prompt emission from the supermassive collapsar jets. Since the emission mechanisms of the prompt emission of GRBs are still under debates, however, following Nakauchi et al. (2012), we evaluate them by applying simple empirical relations to supermassive collapsar jets.

First of all, we describe our model for the prompt emission. We assume that once the jet breaks out the surface at t_b , the relativistic jet can contribute to the gamma-ray emission by using a fraction ϵ_γ of its energy. Thus, the collimation-corrected gamma-ray luminosity is given by $L_\gamma(t) = \epsilon_\gamma L_j(t)$. We also assume that the high energy emission lasts until all the matter in the envelope has accreted onto the central BH at $t_{\text{ff},*} = t_{\text{ff}}(R_*)$. Hence, the duration of the prompt emission can be evaluated by $t_{\text{ff},*} - t_b$. Hereafter, we adopt $\theta = 5^\circ$, $\epsilon_\gamma = 0.1$ and $\eta_j = 6.2 \times 10^{-4}$ as our fiducial values. Then the isotropic luminosity of the prompt emission is given by $L_{\gamma,\text{iso}}(t) = \frac{2}{\theta^2} \epsilon_\gamma \eta_j \dot{M}(t) c^2$. In this model, the isotropic radiated energy of the prompt emission $E_{\gamma,\text{iso}}$ and the peak luminosity L_p are estimated by

$$\begin{aligned} E_{\gamma,\text{iso}} &= \frac{2}{\theta^2} \int_{t_b}^{t_{\text{ff},*}} L_\gamma(t) dt = \frac{2}{\theta^2} \epsilon_\gamma \eta_j c^2 \int_{t_b}^{t_{\text{ff},*}} \dot{M}(t) dt \\ &= 2.9 \times 10^{52} \left(\frac{\int_{t_b}^{t_{\text{ff},*}} \dot{M} dt}{1 M_\odot} \right) \text{ergs}, \end{aligned} \quad (16)$$

and

$$\begin{aligned} L_p &= L_{\gamma,\text{iso}}(t = t_b) = \frac{2}{\theta^2} \epsilon_\gamma \eta_j c^2 \dot{M}(t = t_b) \\ &= 2.9 \times 10^{52} \left(\frac{\dot{M}(t = t_b)}{1 M_\odot \text{ s}^{-1}} \right) \text{ergs s}^{-1}. \end{aligned} \quad (17)$$

As long as the luminosity is proportional to the mass accretion rate, the luminosity decreases monotonically after the breakout. Therefore, the luminosity peaks at the breakout.

Next, we evaluate the spectral peak energy of the prompt emission in the central-engine frame E_p . Following Nakauchi et al. (2012), we assume that either one of the two empirical correlations of LGRBs holds in supermassive collapsar jets: the E_p - L_p correlation or the E_p - $E_{\gamma,\text{iso}}$ correlation (Yonetoku et al. 2004; Amati et al. 2002). If the E_p - L_p correlation holds for the burst, then the spectral peak energy can be evaluated from the peak luminosity L_p , using the correlation

$$\frac{L_p}{10^{52} \text{ erg s}^{-1}} \simeq 2 \times 10^{-5} \left(\frac{E_p}{1 \text{ keV}} \right)^{2.0}, \quad (18)$$

as $E_p = 5.6 \times 10^2$ and 1.6×10^2 keV for the 1E5 model and the 1E4 model, respectively. On the other hand, if the E_p - $E_{\gamma,\text{iso}}$ correlation holds for the burst, E_p can be evaluated from the isotropic radiated energy $E_{\gamma,\text{iso}}$, using the correlation

$$\frac{E_p}{1 \text{ keV}} \simeq 80 \left(\frac{E_{\gamma,\text{iso}}}{10^{52} \text{ erg}} \right)^{0.57}, \quad (19)$$

as $E_p = 2.6 \times 10^4$ and 1.4×10^4 keV for the 1E5 model

Table 1
Observational Characteristics of the Prompt Emission at $z = 15$

Progenitor Model	1E5	1E4
$E_{\gamma,\text{iso}}$ [erg]	2.5×10^{56}	8.4×10^{55}
L_p [erg s $^{-1}$]	6.2×10^{52}	5.1×10^{51}
E_p^{obs} [keV]	3.5×10	1.0×10
E_p^{obs} [keV]	1.6×10^3	8.6×10^2

Notes. E_p^{obs} in line 4 and E_p^{obs} in line 5 show the peak energy of the spectrum predicted by the empirical relations (18) and (19), respectively.

and the 1E4 model, respectively. We summarize the observational signatures of the prompt emission from the supermassive collapsar jets in Table 1, where the redshift of the burst is set as $z = 15$. In lines 4 and 5, the spectral peak energy in the observer frame E_p^{obs} is given by $E_p^{\text{obs}} = E_p/(1+z)$. From Table 1, we find that the total energy is much larger than that of LGRBs, while the peak luminosity is comparable to them. The accretion time of SMS is much longer than that of LGRB so that SMS releases much larger amount of energy than WR collapsars although the luminosity is similar.

Finally, we discuss the detectability of the prompt emission from the supermassive collapsar jet with detectors like the Burst Alert Telescope (BAT) on board the *Swift* satellite (Barthelmy et al. 2005). BAT covers the energy range from $E_{\text{min}} = 15$ keV to $E_{\text{max}} = 150$ keV. The energy flux detected by BAT is given by

$$f_{\text{sig}}(t_{\gamma,\text{obs}}) = F_{\text{bol}}(t_\gamma) \frac{\int_{E_{\text{min}}}^{E_{\text{max}}} EN(E) dE}{\int_0^\infty EN(E) dE}, \quad (20)$$

where $t_\gamma = t - t_b$, $t_{\gamma,\text{obs}} = (1+z)t_\gamma$, $N(E)$ and $F_{\text{bol}}(t_\gamma)$ are the time from the breakout, the time in the observer frame, the photon number spectrum and the bolometric flux, respectively. Empirically, we assume that $N(E)$ is represented by the Band function (Band et al. 1993) with the spectral indices of $\alpha = -1$ and $\beta = -2.3$ (Kaneko et al. 2006). The bolometric flux is given by

$$F_{\text{bol}}(t_{\gamma,\text{obs}}) = \frac{L_{\gamma,\text{iso}}(t_\gamma)}{4\pi d_L(z)^2} \text{erg s}^{-1} \text{ cm}^{-2}, \quad (21)$$

where $d_L(z)$ is the luminosity distance.

In Figure 4, we show the light curves of the prompt emission in the case of the E_p - L_p correlation. The red and blue curves correspond to the 1E5 and the 1E4 models, respectively. We set the redshifts of the bursts as $z = 10$ (solid), 15 (dash-dotted), 20 (dotted), respectively. The gray dotted lines show the BAT sensitivities $f_{\text{sen}}(\Delta t_{\text{obs}})$ with the integration times of $\Delta t_{\text{obs}} = 1$ s, 10^2 s, and 10^4 s, from top to bottom. If the burst enters the field of view of the BAT at some time $t_{\gamma,\text{obs}}$, and the signal flux is larger than $f_{\text{sen}}(\Delta t_{\text{obs}})$, then it can be observed by BAT up to $t_{\gamma,\text{obs}} + \Delta t_{\text{obs}}$. We can see that the burst can be detectable up to $z = 20$ for $\Delta t_{\text{obs}} = 10^2$ s in the 1E5 model. We can also see that the burst can be detectable up to $z = 20$ for $\Delta t_{\text{obs}} = 10^4$ s in the 1E4 model.

In Figure 5, we show the light curves of the burst in the case of the E_p - $E_{\gamma,\text{iso}}$ correlation. We can see that the observed flux is smaller by an order of magnitude

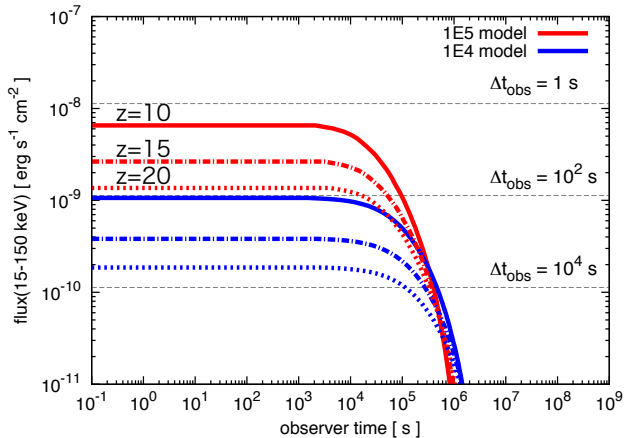


Figure 4. Light curves of the prompt emission of the ULGRBs from supermassive collapsars. The flux is calculated at the *Swift* BAT energy range (15-150 keV), assuming that the E_p - L_p correlation holds. The red and blue curves correspond to the 1E5 and the 1E4 models, respectively. The redshifts of the bursts are $z = 10$ (solid), 15 (dash-dotted), 20 (dotted), respectively. The gray dotted lines show the BAT sensitivities $f_{\text{sen}}(\Delta t_{\text{obs}})$ with the integration times of $\Delta t_{\text{obs}} = 1, 10^2, 10^4$ s, from up to bottom.

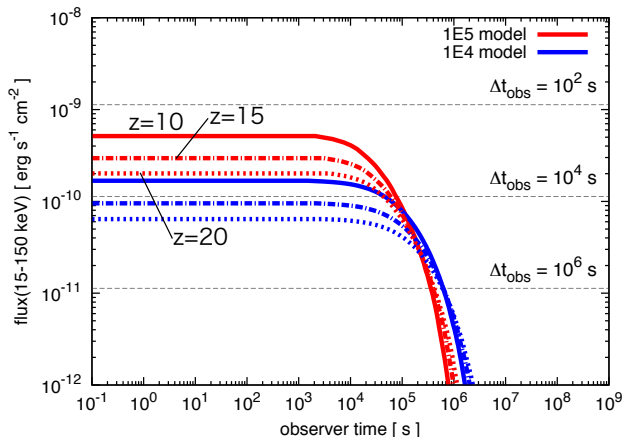


Figure 5. The same as Figure 4, but the flux is calculated assuming that the E_p - $E_{\gamma,\text{iso}}$ correlation holds.

than that of the above case. This is because the E_p - $E_{\gamma,\text{iso}}$ correlation leads to $E_p^{\text{obs}} \simeq 1$ MeV, which is out of the BAT energy range. Nonetheless, we can see that the burst can be detectable up to $z = 20$ for $\Delta t_{\text{obs}} = 10^4$ s in the 1E5 model. On the other hand, in the 1E4 model, longer integration times ($\Delta t_{\text{obs}} > 10^4$ s) are needed to detect the burst at such a high redshift of 20.

Thus, we conclude that the prompt emission from supermassive collapsar jets can be detectable as ULGRBs up to $z \sim 20$ even with the current detectors like BAT.

5. DISCUSSION

5.1. Accreting supermassive stars

If the high mass accretion rate of 0.1 - $1 M_{\odot} \text{ yr}^{-1}$ continues, the SMS mass will eventually reach a few times $\sim 10^5 M_{\odot}$ and the GR instability sets in to lead the for-

mation of a BH and accretion disk system¹². Such a high mass accretion rate onto protostars is obtained if the temperature is high as shown in Equation (1) and second paragraph of Section 2. Recently, Hosokawa et al. (2013) calculated the evolution of a SMS under such a high mass accretion rate ~ 0.1 - $1 M_{\odot} \text{ yr}^{-1}$ from the protostar phase to the final mass of $M_* = 10^5 M_{\odot}$. They found that the SMS evolves with a very large envelope of the stellar envelope has a large opacity dominated by H^- ions, and absorbs heat released by the contraction of the stellar inner region. Then, the stellar envelope expands as the protostar accretes matter (Hosokawa et al. 2012).

Hosokawa et al. (2013), however, were not able to compute the SMS evolution beyond $10^5 M_{\odot}$, because their stellar evolution code is suffered from the numerical difficulties. The reason is not clear. If the accretion is stopped before the GR instability sets in, the final pre-collapse model is similar to the 1E5 model so that the ULGRB of the SMS is expected as discussed in the previous section. If the accretion continues, the SMS will enter the GR instability region. In such a case, we can assume that the SMS has similar density profile obtained by Hosokawa et al. (2013) when it begins to collapse through the GR instability. The structure of the SMS envelope would not change so much as long as the high mass accretion rate is kept until the SMS obtains the critical mass. Therefore, our assumption may be justified for the envelope, which is important for the propagation of jet heads as we saw in the previous section.

In Figure 6, we show the density profile of the accreting SMS when its mass reaches $M_* = 10^5 M_{\odot}$ by using the magenta curve. While in Hosokawa et al. (2013), the density profile is given as a function of the mass coordinate M_r (in Fig. 3 of their paper), we show it as a function of radius r by integrating the mass conservation equation $dr/dM_r = 1/4\pi r^2 \rho(M_r)$. As shown in Figure 6, the accreting SMS is about 10 times larger than a RSG. Hence one may expect that the jet can not break out the surface of the star as RSGs. However, we find this progenitor also has a steep density profile in the radiation-pressure-dominated envelope. Therefore, according to the argument in Section 4.1, we expect that a relativistic jet is accelerated to break out the surface of the progenitor star. We calculate the jet propagation in the same way described in Section 3, and find that the jet actually breaks out the envelope. Thus, we expect that even if the SMS collapses in the accreting protostar phase, it can produce an energetic explosion. We also calculate light curves of the prompt emission, assuming that the E_p - L_p and the E_p - $E_{\gamma,\text{iso}}$ correlations hold. In Figures 7 and 8, we show the light curves. ULGRBs from accreting SMSs are dimmer than the GRBs from the 1E5 model. This is because the accreting SMSs are larger than SMSs of the 1E5 model. It takes more time for a jet to break out the larger envelope. Thus, when the jet breaks out

¹² If a SMS rotates, it is stabilized against the GR instability (e.g., Fowler 1966; Bisnovatyi-Kogan et al. 1967; Baumgarte & Shapiro 1999). However, even if the SMS rotates, it will not acquire more mass than $\sim 10^6 M_{\odot}$ for the highest mass accretion rate of $1 M_{\odot} \text{ s}^{-1}$. Eventually, it exhausts the nuclear fuel in ~ 1 Myr and collapses to form the central BH. Actually, the calculation of Hosokawa et al. (2013) shows that the hydrogen burning occurs in the core.

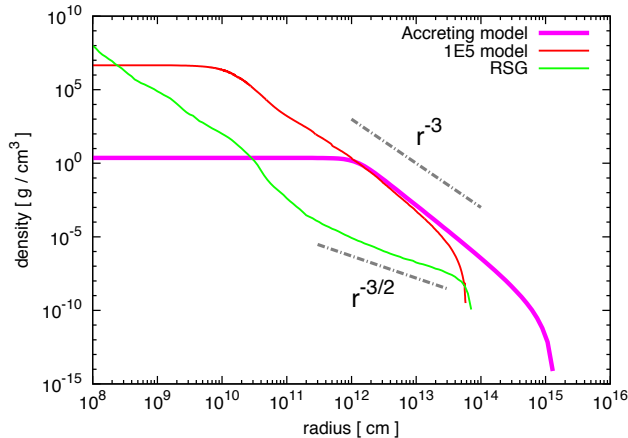


Figure 6. Density profile of an accreting SMS with mass of $10^5 M_\odot$ (magenta curve). This progenitor also has the steep density profile of the envelope (with slope of ~ 3), where a relativistic jet is not decelerated. Note that this progenitor is not yet in the pre-collapse phase, but in the accreting protostar phase. We can expect that when the GR instability sets in, however, the pre-collapse progenitor has the similar density profile especially in the envelope as long as the high mass accretion rate is kept. With the red and green curves, we also show the density profiles of the 1E5 model and RSG, respectively, for references as in Figure 1.

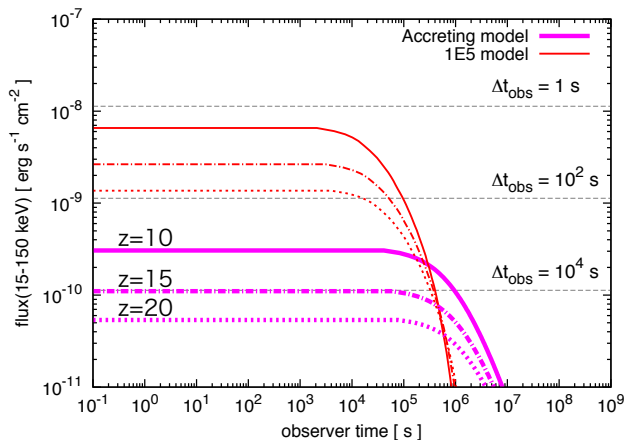


Figure 7. The same as Figure 4, but the flux is calculated from the accreting supermassive collapsar (magenta curves) assuming that the E_p - L_p correlation holds. We also show the light curves of the 1E5 model for references.

the envelope, the accretion rate onto the central BH is decreased. The observation time to detect ULGRBs from accreting SMSs is longer than that of the non-accreting SMSs in Figures 4 and 5.

5.2. Event Rate

We briefly discuss the detection rate of the ULGRBs from supermassive collapsars. For a given observation time Δt_{obs} , the cumulative number of ULGRBs $\Delta N(z)$ which have redshifts less than z can be calculated from

$$\Delta N(z) = \int_0^z \Psi_{\text{GRB}}(z') 4\pi cr(z')^2 \left| \frac{dt}{dz} \right| dz' \Delta t_{\text{obs}}, \quad (22)$$

where Ψ_{GRB} is the intrinsic event rate of ULGRBs and $r(z)$ is the comoving distance to the redshift z . While the intrinsic event rate Ψ_{GRB} is still uncertain, we can

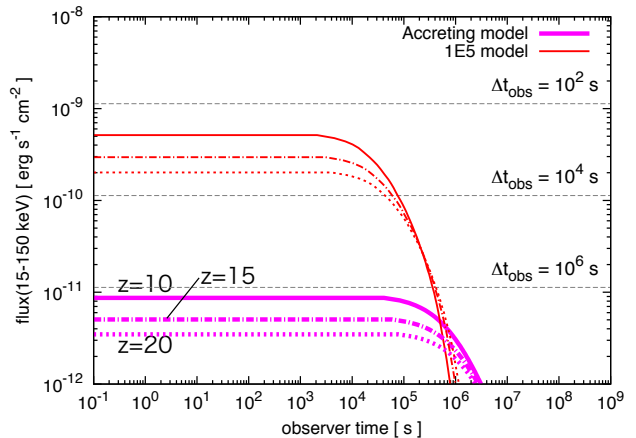


Figure 8. The same as Figure 7, but the flux is calculated assuming that the E_p - $E_{\gamma, \text{iso}}$ correlation holds.

roughly estimate it by using the formation rate of SMSs or DCBHs, which are theoretically studied in the previous studies (Agarwal et al. 2012; Dijkstra et al. 2014; Yue et al. 2014).

Yue et al. (2014) studied the formation rate of DCBHs in the early Universe. They found that DCBHs can be formed from $z = 20$ to 13 (corresponding to ~ 150 Myr), and that the comoving mass density of DCBHs can be $\rho_{\text{DCBH}} \sim 2 \times 10^6 M_\odot \text{Mpc}^{-3}$. Since they assumed the typical mass of a DCBH as $M_{\text{DCBH}} \sim 10^6 M_\odot$, the comoving number density of DCBHs can be evaluated as $n_{\text{DCBH}} \sim \rho_{\text{DCBH}}/M_{\text{DCBH}} \sim 2 \text{Mpc}^{-3}$.¹³ Then, we can obtain the intrinsic rate of ULGRBs as $\Psi_{\text{GRB}} \sim 2 \text{Mpc}^{-3}/150 \text{Myr} \sim 10^{-8} \text{yr}^{-1} \text{Mpc}^{-3}$. It should be noted that in this rough estimate, we assume that all the SMSs collapse to DCBHs after they contribute to ULGRBs. This rate may be optimistic.

Substituting the above value into Equation (22), the event rate of the ULGRBs on the whole sky can be obtained as

$$\begin{aligned} \frac{\Delta N}{\Delta t_{\text{obs}}} &= \int_{z=13}^{z=20} \Psi_{\text{GRB}}(z') 4\pi cr(z')^2 \left| \frac{dt}{dz} \right| dz' \\ &\sim 6 \times 10^2 \left(\frac{\Psi_{\text{GRB}}}{10^{-8} \text{yr}^{-1} \text{Mpc}^{-3}} \right) \text{yr}^{-1}. \quad (23) \end{aligned}$$

The detection rate of the ULGRBs is reduced by the beaming factor, $\Omega_{\text{beam}} := \theta^2/2 \simeq 3.8 \times 10^{-3} (\theta/5^\circ)^2$, since the off-axis bursts are not detectable. By multiplying the beaming factor to Equation (23), the detection rate is about one event per year.

The emission from an expanding cocoon fireball might play a key role to raise the detection rate of the event. After the jet breakout, the cocoon also breaks out the star and evolves like a non-relativistic fireball outside the star (Kashiyama et al. 2013; Nakauchi et al. 2013). The cocoon emission will be isotropic and free from the beaming effect.

¹³ This number density seems larger than that of the observed typical galaxies. In Yue et al. (2014), however, they discussed that only a fraction of DCBHs can grow up by the mass accretion and that most DCBHs do not acquire sufficient mass and escape our observation.

5.3. Feedback Effects on the Surrounding Environments

Various feedback effects are expected from the supermassive collapsars, since they release a huge amount of energy. In fact, the total energy of the cocoon fireball discussed above could be as large as $E_c \sim 10^{55}$ - 10^{56} erg, which can be calculated from Equation (10), $E_c = E_c(t = t_b)$. Then, the emission from the cocoon fireball might be observed as the most energetic supernova explosions in the Universe. Moreover, such a violent explosion could disrupt the host halo, and hinder the remnant massive BHs from growing up to SMBHs within $\lesssim 1$ Gyr after the BH formation.

In addition, if heavy elements are produced in the jet head and cocoon, they could contribute to the chemical enrichment of the host halo. The metal polluted gas will induce the formation of second generation of stars. The line features in the cocoon emission could also tell us the abundance pattern of the nucleosynthesis to confirm the SMS origin, although the line may be broad due to the high expansion velocity.

Recently, Johnson et al. (2013) and Whalen et al. (2013) considered a very energetic supernova explosion of $\sim 10^{55}$ erg in the first galaxies, and calculated the dynamical evolution of the blast wave within the host. They found that whereas the blast wave engulfs the entire galaxy, most of its energy is radiated away via efficient cooling processes, so that the swept up matters ($\sim 10^7 M_\odot$) could recollapse to the host ~ 70 Myr after the explosion. Thus, such an energetic explosion might not hinder the remnant massive BH from becoming supermassive within $\lesssim 1$ Gyr after its formation. On the other hand, the momentum conservation suggests that the host galaxy is expelled if the explosion energy is larger than $\sim 10^{56} (M_{\text{halo}}/10^7 M_\odot)(v_{\text{esc}}/10 \text{ km s}^{-1})(\beta_c/0.3)$ erg. Thus more detailed calculations are worth while.

Even after contributing to the prompt emission, the relativistic jet has a huge amount of kinetic energy $E_{\text{k,iso}} = E_{\gamma,\text{iso}}(1 - \epsilon_\gamma)/\epsilon_\gamma \sim 10^{57}$ erg. This can lead to bright afterglow emissions at various wavelengths (Toma et al. 2011; Ioka & Mészáros 2005). The detection of such afterglow emissions could provide us rich information about the surrounding environments of SMSs such as the density and the chemical composition of the circumstellar medium.

6. SUMMARY AND CONCLUSIONS

We investigated whether in the early Universe SMSs are able to produce GRBs according to the collapsar scenario. Since SMSs have radii at least as large as RSGs, naively it would seem difficult for a relativistic jet to reach the surface before the jet engine dies. Actually calculating the jet propagation in SMSs, however, we find that jets are able to break out the thick envelope of SMSs. This is because the envelope of SMSs is dominated by radiation pressure and has a steeper density gradient than RSGs in which the gas pressure dominates. Our conclusion is that SMSs forming in protogalaxies can produce violent GRBs.

Based on empirical rules, we find that the collapse of SMSs may be observed as ULGRBs with a duration of $\sim 10^4$ - 10^6 s by the current detectors like BAT. Our optimistic estimates indicate rates of detectable GRBs of

about one event per year. Comparing with observations, we can impose some conditions on the intrinsic event rate which is related to the SMS or DCBH formation rate. Since GRBs are collimated bursts, beaming reduces the rate of detectable events. Therefore, it is important to consider the isotropic emission accompanying GRBs, e.g., the cocoon fireball emissions. Studying the detectability of cocoon fireball emission is an interesting future work.

The SMS GRBs are very energetic explosions releasing more than 10^{55} - 10^{56} erg and sweep up or blow off the matter in protogalaxies. As a result, GRBs strongly influence the mass accretion onto the newborn seed BHs. This negative feedback needs to be taken into account when studying the growth of remnant BHs.

ACKNOWLEDGMENTS

We thank T. Hosokawa, K. Kashiyama and K. Inayoshi for fruitful discussions and comments. This work is supported in part by the Grant-in-Aid from the Ministry of Education, Culture, Sports, Science and Technology (MEXT) of Japan, Nos. 261051 (DN) 24103006, 26287051, 24000004, 26247042 (KI) 24103006, 15H02087(TN). AH was supported by an Australian Research Council (ARC) Future Fellowship (FT120100363) and NSF grant PHY-1430152 (JINA-CEE).

REFERENCES

- Agarwal, B., Khochfar, S., Johnson, J. L., et al. 2012, MNRAS, 425, 2854
- Alvarez, M. A., Wise, J. H., & Abel, T. 2009, ApJ, 701, L133
- Amati, L., Frontera, F., Tavani, M., et al. 2002, A&A, 390, 81
- Band, D., Matteson, J., Ford, L., et al. 1993, ApJ, 413, 281
- Barkov, M. V. 2010, Astrophys. Bull., 65, 217
- Barthelmy, S. D., Barbier, L. M., Cummings, J. R., et al. 2005, Space Sci. Rev., 120, 143
- Baumgarte, T. W., & Shapiro, S. L. 1999, ApJ, 526, 941
- Begelman, M. C., & Cioffi, D. F. 1989, ApJ, 345, L21
- Begelman, M. C., Rossi, E. M., & Armitage, P. J. 2008, MNRAS, 387, 1649
- Bisnovatyi-Kogan, G. S., Zel'dovich, Y. B., & Novikov, I. D. 1967, Soviet Ast., 11, 419
- Blandford, R. D., & Znajek, R. L. 1977, MNRAS, 179, 433
- Bromberg, O., Nakar, E., Piran, T., & Sari, R. 2011, ApJ, 740, 100
- Bromm, V., & Loeb, A. 2003, ApJ, 596, 34
- Chen, K.-J., Heger, A., Woosley, S., et al. 2014, ApJ, 790, 162
- Chandrasekhar, S. 1964, ApJ, 140, 417
- Czerny, B., Janiuk, A., Sikora, M., & Lasota, J. P. 2012, ApJ, 755, L15
- Dijkstra, M., Ferrara, A., & Mesinger, A. 2014, MNRAS, 442, 2036
- de Souza, R. S., Yoshida, N., & Ioka, K. 2011, A&A, 533, A32
- Fowler, W. A. 1966, ApJ, 144, 180
- Fryer, C. L., & Heger, A. 2011, Astronomische Nachrichten, 332, 408
- Fryer, C. L., Woosley, S. E., & Heger, A. 2001, ApJ, 550, 372
- Fan, X. 2006, New A Rev., 50, 665
- Frail, D. A., Kulkarni, S. R., Sari, R., et al. 2001, ApJ, 562, L55
- Gaspari, M., Ruszkowski, M., & Oh, S. P. 2013, MNRAS, 432, 3401
- Gendre, B., Stratta, G., Atteia, J. L., et al. 2013, ApJ, 766, 30
- Haiman, Z. 2013, Astrophysics and Space Science Library, 396, 293
- Hjorth, J., & Bloom, J. S. 2012, Chapter 9 in "Gamma-Ray Bursts", Cambridge Astrophysics Series 51, eds. C. Kouveliotou, R. A. M. J. Wijers and S. Woosley, Cambridge University Press (Cambridge), p. 169-190, 169
- Hirano, S., Hosokawa, T., Yoshida, N., et al. 2014, ApJ, 781, 60
- Hosokawa, T., Omukai, K., & Yorke, H. W. 2012, ApJ, 756, 93
- Hosokawa, T., Yorke, H., Inayoshi, K., Omukai, K., & Yoshida, N. 2013, ApJ, 778, 178
- Inayoshi, K., Omukai, K., & Tasker, E. 2014, MNRAS, 445, L109
- Ioka, K., & Mészáros, P. 2005, ApJ, 619, 684
- Jiang, Y.-F., Stone, J. M., & Davis, S. W. 2014, ApJ, 796, 106

- Johnson, J. L., Whalen, D. J., Agarwal, B., Paardekooper, J.-P., Khochfar, S. 2014, *MNRAS*, 445, 686
- Johnson, J. L., Whalen, D. J., Even, W., et al. 2013, *ApJ*, 775, 107
- Kashiyama, K., Nakauchi, D., Suwa, Y., Yajima, H., & Nakamura, T. 2013, *ApJ*, 770, 8
- Kaneko, Y., Preece, R. D., Briggs, M. S., et al. 2006, *ApJS*, 166, 298
- Kippenhahn, R., & Weigert, A. 1990, *Stellar Structure and Evolution*, XVI, 468 pp. 192 figs.. Springer-Verlag Berlin Heidelberg New York. Also *Astronomy and Astrophysics Library*
- Komissarov, S. S., & Barkov, M. V. 2010, *MNRAS*, 402, L25
- Kouveliotou, C., Meegan, C. A., Fishman, G. J., et al. 1993, *ApJ*, 413, L101
- Kumar, P., Narayan, R., & Johnson, J. L. 2008, *MNRAS*, 388, 1729
- Latif, M. A., Schleicher, D. R. G., Schmidt, W., & Niemeyer, J. 2013, *MNRAS*, 433, 1607
- Levan, A. J., Tanvir, N. R., Starling, R. L. C., et al. 2014, *ApJ*, 781, 13
- MacFadyen, A. I., & Woosley, S. E. 1999, *ApJ*, 524, 262
- Madau, P., & Rees, M. J. 2001, *ApJ*, 551, L27
- Matzner, C. D. 2003, *MNRAS*, 345, 575
- Matzner, C. D., & McKee, C. F. 1999, *ApJ*, 510, 379
- Mizuta, A., & Ioka, K. 2013, *ApJ*, 777, 162
- Mortlock, D. J., Warren, S. J., Venemans, B. P., et al. 2011, *Nature*, 474, 616
- Nagakura, H., Suwa, Y., & Ioka, K. 2012, *ApJ*, 754, 85
- Nakauchi, D., Suwa, Y., Sakamoto, T., Kashiyama, K., & Nakamura, T. 2012, *ApJ*, 759, 128
- Nakauchi, D., Kashiyama, K., Suwa, Y., & Nakamura, T. 2013, *ApJ*, 778, 67
- Omukai, K. 2001, *ApJ*, 546, 635
- Osaki, Y. 1966, *PASJ*, 18, 384
- Planck Collaboration, Ade, P. A. R., Aghanim, N., et al. 2015, arXiv:1502.01589
- Popham, R., Woosley, S. E., & Fryer, C. 1999, *ApJ*, 518, 356
- Quataert, E., & Kasen, D. 2012, *MNRAS*, 419, L1
- Sądowski, A., Narayan, R., McKinney, J. C., & Tchekhovskoy, A. 2014, *MNRAS*, 439, 503
- Shakura, N. I., & Sunyaev, R. A. 1973, *A&A*, 24, 337
- Shang, C., Bryan, G. L., & Haiman, Z. 2010, *MNRAS*, 402, 1249
- Shapiro, S. L., & Teukolsky, S. A. 1983, *Research supported by the National Science Foundation*. New York, Wiley-Interscience, 1983, p. 663
- Shibata, M., & Shapiro, S. L. 2002, *ApJ*, 572, L39
- Susa, H., Hasegawa, K., & Tominaga, N. 2014, *ApJ*, 792, 32
- Suwa, Y., & Ioka, K. 2011, *ApJ*, 726, 107
- Toma, K., Sakamoto, T., & Mészáros, P. 2011, *ApJ*, 731, 127
- Volonteri, M., & Rees, M. J. 2005, *ApJ*, 633, 624
- Whalen, D. J., Johnson, J. L., Smidt, J., et al. 2013, *ApJ*, 777, 99
- Wu, X.-B., Wang, F., Fan, X., et al. 2015, *Nature*, 518, 512
- Woosley, S. E., 1993, *ApJ*, 405, 273
- Woosley, S. E., & Bloom, J. S. 2006, *ARA&A*, 44, 507
- Woosley, S. E., & Heger, A. 2012, *ApJ*, 752, 32
- Woosley, S. E., & Heger, A. 2015, *ApJ*, 806, 145
- Woosley, S. E., Heger, A., & Weaver, T. A. 2002, *Reviews of Modern Physics*, 74, 1015
- Yonetoku, D., Murakami, T., Nakamura, T., et al. 2004, *ApJ*, 609, 935
- Yue, B., Ferrara, A., Salvaterra, R., Xu, Y., & Chen, X. 2014, *MNRAS*, 440, 1263